Article

Adsorption and Sensing Properties of Dissolved Gas in Oil on Cr-Doped InN Monolayer: A Density Functional Theory Study

Guochao Qian [1,2], Jin Hu [1], Shan Wang [1], Weiju Dai [1] and Qu Zhou [3,*]

[1] Electric Power Science Research Institute of Yunnan Power Grid Co., Ltd., Kunming 650214, China; zm18973102153@163.com (G.Q.); i23456789jkl@163.com (J.H.); ws1smirage@sina.com (S.W.); dwj0479@163.com (W.D.)
[2] State Key Laboratory of Power Transmission Equipment and System Security and New Technology, Chongqing University, Chongqing 400044, China
[3] College of Engineering and Technology, Southwest University, Chongqing 400715, China
* Correspondence: zhouqu@swu.edu.cn

Abstract: Dissolved gas analysis (DGA) is recognized as one of the most reliable methods in transformer fault diagnosis technology. In this paper, three characteristic gases of transformer oil (CO, C_2H_4, and CH_4) were used in conjunction with a Cr-decorated InN monolayer according to first principle calculations. The adsorption performance of Cr–InN for these three gases were studied from several perspectives such as adsorption structures, adsorption energy, electron density, density of state, and band gap structure. The results revealed that the Cr–InN monolayer had good adsorption performance with CO and C_2H_4, while the band gap of the monolayer slightly changed after the adsorption of CO and C_2H_4. Additionally, the adsorption property of the Cr–InN monolayer on CH_4 was acceptable and a significant response was simultaneously generated. This paper provides the first insights regarding the possibility of Cr-doped InN monolayers for the detection of gases dissolved in oil.

Keywords: DFT; DGA; inn monolayer; adsorption; gas sensors

1. Introduction

The power transformer is one of the most essential pieces of hinge equipment of an electrical power system [1]. There are still a considerable number of large and medium-sized transformers around the world that use transformer oil as a cooling and insulating medium [2]. Effectively detecting the operating status of oil-immersed transformers to discover insulation defects in advance and eliminate hidden troubles in time can help to ensure the stable running of a power system [3,4].

Dissolved gas analysis (DGA) is considered to be a reliable method for monitoring the operating status of transformers; the prevailing approach is to determine the content of dissolved gases in the insulating oil through gas chromatography to find out whether there are potential overheating and discharge faults in the running transformer equipment [5,6]. In addition, the gas sensor has attracted the attention of many scholars due to its low cost, simple operation process, and many other advantages. The selection of gas-sensing materials determines the performance of gas-sensing sensors, so it has always been a hot topic to explore novel and excellent-performance gas-sensing materials.

Among the different kinds of gas-sensitive materials, two-dimensional (2D) materials stand out for their excellent characteristics [7–13], such as large specific surface area, extraordinary electronic mobility, and chemical activity, which meet the prerequisites for the exploitation of high-sensitivity gas sensor based on 2D materials [14–16]. Indium nitride (InN) is a new type III-nitride group compound material. It has excellent electronic transport performance and a narrow energy band, and has received extensive attention in the field of new optoelectronic device manufacturing. However, to our knowledge, only a

few researchers have focused on 2D InN applications such as gas sensors. For example, it was found by Peng et al. that an Au–InN monolayer acted as the gas adsorbent for SF$_6$, which needed to decompose components to guarantee the stable operation of SF$_6$ insulation equipment [17]. Zhu et al. proved that an InN monolayer doped by the transition metal Pd is an exceptional material for use in detecting NO and CO based on density functional theory (DFT) [18]. It can be seen that 2D InN has potential in the development of gas-sensitive materials. Here, we further explored the gas-sensing mechanism between InN monolayers and other different gases, and we provide preliminary direction for the exploration of InN monolayer gas sensors [19–21].

In this work, DFT calculations were adopted to investigate the adsorption behavior of an InN monolayer to CH$_4$, CO, and C$_2$H$_2$ (three characteristic gases in transformer oil). First, we constructed the optimal Cr-doped InN (Cr–InN) monolayer and carried out adsorption calculations for the different gases based on this model. We collected data on the adsorption parameters, including adsorption energy, the value of charge transfer, and the electron density of each adsorption system, to analyze the changes in the total energy and the charge transfer of the Cr–InN monolayer during the adsorption process. Additionally, we employed total density states (DOS) and partial density states (PDOS) to investigate the variation of the electron states around the Fermi level and the hybridization states in the adsorption systems. Moreover, the band gap structures were identified to qualitatively discuss the conductivity of the adsorption system compared to the isolated Cr–InN monolayer. Through the above calculations and analyses, we were able to determine whether an InN monolayer could be used for detecting these three dissolved gases in oil.

2. Materials and Methods

All DFT spin-unrestricted calculations in this work were performed by Dmol^3 package of Material Studio software [22,23]. The Perdew–Burke–Ernzerhof (PBE) with the generalized gradient approximation (GGA) function was employed to deal with the exchange-correlation between electrons. Double numerical polarization (DNP) was adopted as the basis function set of linear combination of atomic orbitals (LCAO). In order to solve the problem of transition metal in the system, DFT semi-core pseudopotential (DSSP) has been adopted [24–26]. When the energy difference between the two geometric optimizations is extremely small (less than 1.0×10^{-5} Ha), the force on each atom is extremely small (less than 0.002 Ha/Å), or the maximum displacement distance of each atom is extremely small (less than 0.005 Å), geometric optimization relaxation can be used to meet the convergence criterion. Additionally, in order to correct for the influence of van der Waals force, the Grimme method was used in all models. For geometric optimization calculations, a $5 \times 5 \times 1$ k-point was adopted, and a more accurate k-point of $7 \times 7 \times 1$ was used for electronic structure calculations [17]. Moreover, for electron orbit calculation in Dmol^3, only $1 \times 1 \times 1$ k points were available for selection [27].

Adsorption energy (E_{ads}) is the most intuitive parameter of adsorption behavior, and in this paper, the E_{ads} of gas adsorption processes was defined as:

$$E_{ads} = E_{ads\ system} - E_{gas} - E_{monolayer} \tag{1}$$

where E_{gas} and $E_{monolayer}$ represent the energy of the intrinsic monolayer and gas molecule, respectively, and $E_{ads\ system}$ is the total energy of adsorption system.

The Hirschfeld charge method was employed to analyze the charge distribution to obtain the charge transfer (Q_T) because it has been reported that there are many errors in Mulliken charge analysis [28].

3. Results

3.1. Structure of Cr–InN Monolayer

Firstly, we established a two-dimensional InN unit cell, and then we built a $4 \times 4 \times 1$ InN supercell based on the unit cell to obtain the InN monolayer, as exhibited in Figure 1. After optimization, the In–N chemical bond in the InN monolayer was 2.092 Å and the

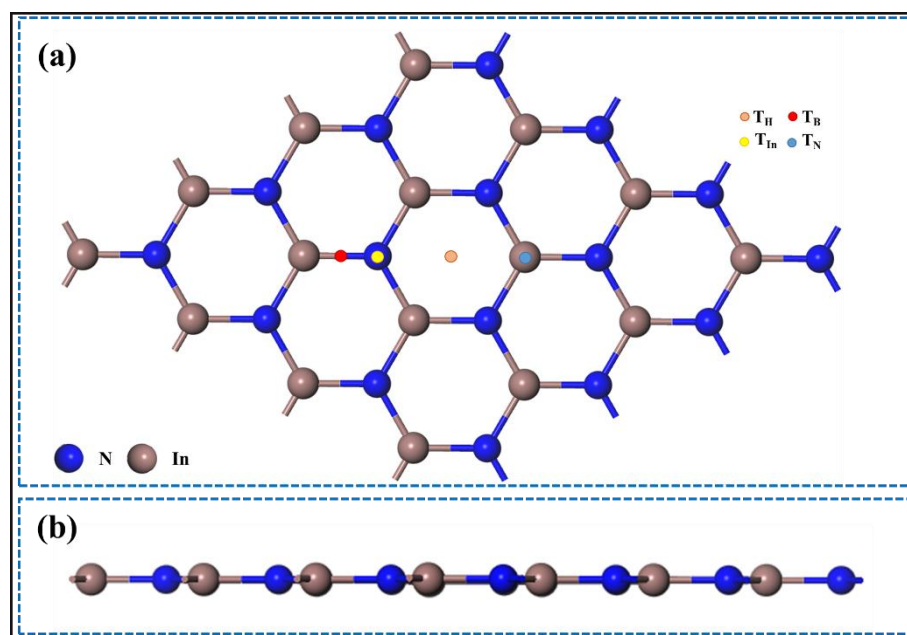lattice parameter value was 3.62 Å, which both corresponded with the results of previous reports [29].

Figure 1. (**a**) Top view and (**b**) side view for geometric construction of the pristine InN monolayer.

There are four possible doping sites on an InN monolayer—the T_H, T_B, T_{In}, and T_N sites [17]. In order to determine the most stable construction of a Cr-doped InN monolayer, four kinds of Cr-decorated InN monolayers based on the abovementioned four doping sites were established; their formation energy and charge transfer were calculated and comprehensively compared to select the most stable doped structure with the best parameters as the basic model for subsequent adsorption calculation. The most stable structure of Cr–InN is exhibited in Figure 2a, which shows that the Cr atom is located at the T_{In} site and the InN monolayer accepts 0.053 e electrons from Cr atoms and forms bonds with Cr atoms, releasing 0.64 eV of energy and indicating that the reaction can spontaneously proceed.
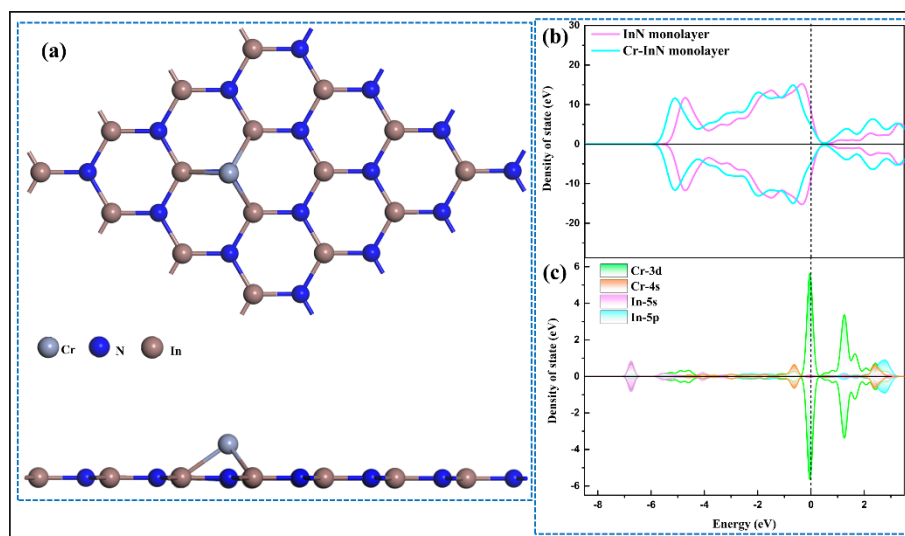

Figure 2. (**a**) Geometric structure, (**b**) TDOS, and (**c**) PDOS of Pd-doped InN monolayer.

DOS analysis was used to explore the effect of Cr atom doping on electronic distribution. It is believed that TDOS can reflect the electron density distribution of a system; as shown in Figure 2b, the electrons of the Cr–InN monolayer moved to a slightly lower energy direction compared to those of the intrinsic InN monolayer. Moreover, some new states were added to the Cr–InN monolayer, which narrowed the intercept near the Fermi level of the TDOS curve of Cr–InN. These phenomena indicate that the introduction of a Cr dopant reduced the intrinsic band gap of InN and improved the electronic activity of the InN monolayer. Regarding PDOS, the overlap between the curves representing the atomic orbitals indicates the orbital hybridization of atoms, which is usually used to explain the bonding between a dopant and intrinsic material (shown in Figure 2c); the overlap between the 5s orbital (In-5s) of the In atom and the Cr-3d orbital at –7 eV and the overlap between the In-5p orbital and the Cr-4s orbital in the range from 1 to 4 eV indicate strong orbital hybridization between these two atoms, thus demonstrating that Cr atoms have been successfully incorporated into the InN monolayer system.

3.2. Geometric Structures and Adsorption Energy Analysis for Adsorption System

We established and optimized the molecular models of CH_4, CO, and C_2H_4 in $Dmol^3$, and we carried out adsorption calculations based on the Cr–InN model constructed above. It is obvious that there were many possible ways for each gas to adsorb on the Cr–InN monolayer. In order to figure out the optimal adsorption structure of each gas, different approaching atoms and adsorption angles were used to obtain all possible adsorption structures, the E_{ads} and Q_t of which were compared. The selected adsorption structures for the three gases with the optimal parameters in the system are shown in Figure 3, and the E_{ads} and adsorption distance corresponding to each structure are shown in Figure 4.

CO and C_2H_4 all were found to be quite close to the Cr atoms of the Cr–InN monolayer; the adsorption distance were 1.85 and 1.794 Å, respectively. At the same time, the absolute values of E_{ads} of these two adsorption systems were quite large, reaching -5.074 and -6.093 eV, respectively. These phenomena preliminarily indicate that the Cr–InN monolayer exhibits an extremely strong absorbability of CO and C_2H_4 gases. However, the adsorption ability of InN on CH_4, with an adsorption energy of 0.652 eV, was found to be relatively high, and its adsorption distance was also the largest of the three systems. An additionally interesting phenomenon is that here, the adsorption distance was relatively small in the system with large absolute value of adsorption energy, which might indicate that for an adsorption system, the greater the adsorption energy value, the stronger the interaction force.
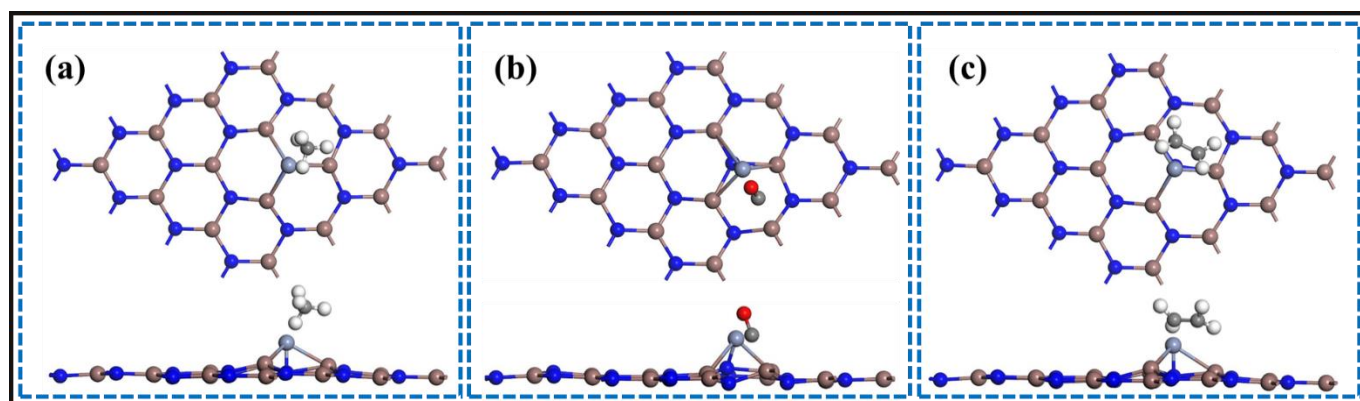

Figure 3. Geometric construction of (**a**) Cr-InN/CH_4, (**b**) Cr-InN/CO, and (**c**) Cr-InN/C_2H_4 adsorption systems.
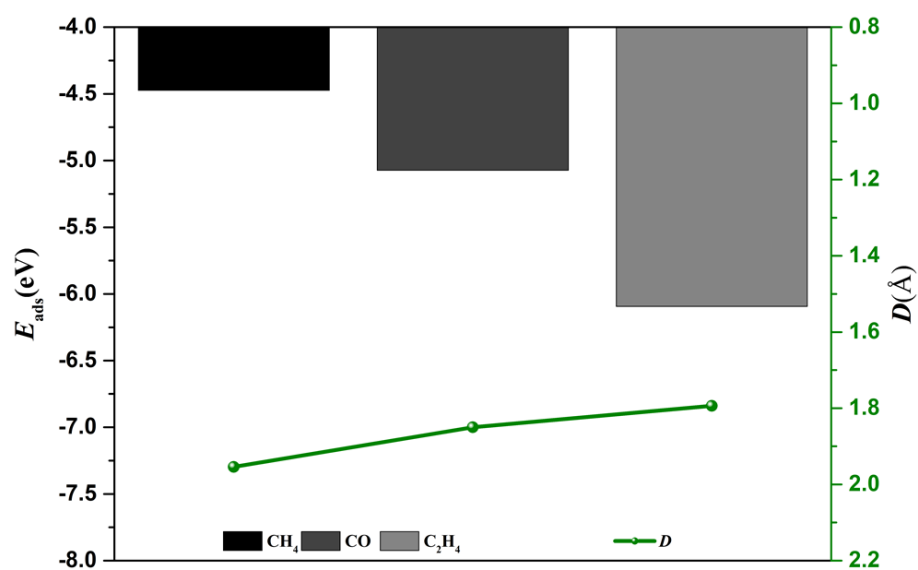
Figure 4. The adsorption energy and adsorption distance of CH_4, CO, and C_2H_4 on the Cr-InN monolayer.

3.3. Electron Density Analysis for Adsorption System

Electron density reveals the probability that electrons are distributed in a particular location surrounding an atom or molecule. By calculating the deformation charge density (DCD), bond formation can intuitively observed and charge transfer can be qualitatively analyzed in an adsorption system [30]. The charge transfer values of CH_4, CO, and C_2H_4 are shown in Table 1, and the deformation charge density is shown in Figure 5.

Table 1. The charge-transfer capacity of CH_4, CO, and C_2H_4 on the Cr–InN monolayer.

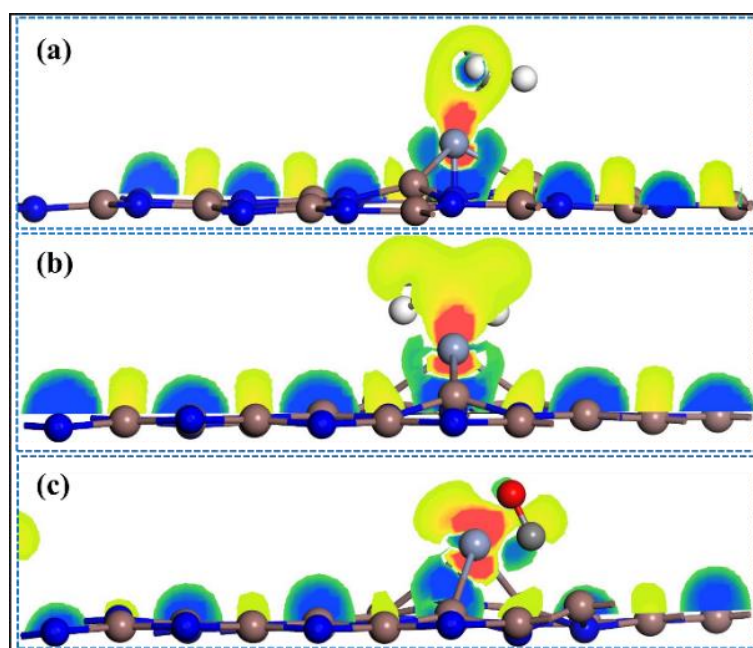| Adsorption System	Q_t (eV)
Pd–SnP$_3$/CO	0.199
Pd–SnP$_3$/CH$_4$	0.052
Pd–SnP$_3$/C$_2$H$_4$	0.204

Figure 5. DCD of (**a**) Cr-InN/CH$_4$, (**b**) Cr-InN/C$_2$H$_4$, and (**c**) Cr-InN/CO adsorption systems.

In each adsorption system, gas molecules acted as reducing agents to transport electrons to the Cr–InN monolayer, that is to say, their charge transfer Q_t was greater than zero. Among them, CO molecules transferred 0.199 e electrons to the Cr–InN monolayer and C_2H_4 molecules transferred 0.204 e electrons to the Cr–InN monolayer. In Figure 5b,c, the red color where the Cr atom is located represents the electron accumulation area, which was almost directly connected to the electron depletion area where the gas molecules were located. This phenomenon shows that there were extremely close charge transfers from gas molecules to the Cr–InN monolayer in the two abovementioned adsorption systems, and strong chemical bonds were formed between C_2H_4, CO molecules and the Cr–InN monolayer. The electron exchange between CH_4 and the Cr–InN monolayer was found to be extremely scarce, and it can be considered that the interaction between the gas molecules and the monolayer was only weak physical adsorption.

3.4. DOS Analysis for Adsorption System

To further strengthen the persuasiveness of the occurred interaction between the Cr–InN monolayer and three gas molecules, TDOS and PDOS (as shown in Figure 6) analyses of each system were conducted to explore the impact of adsorption behavior on the electronic structure of the Cr–InN system. In the TDOS plots, the red curve signals the TDOS of the initial Cr–InN monolayer and the blue displays the system after gas adsorption [10]. In the PDOS plots, several atomic orbitals are represented by areas with different colors.
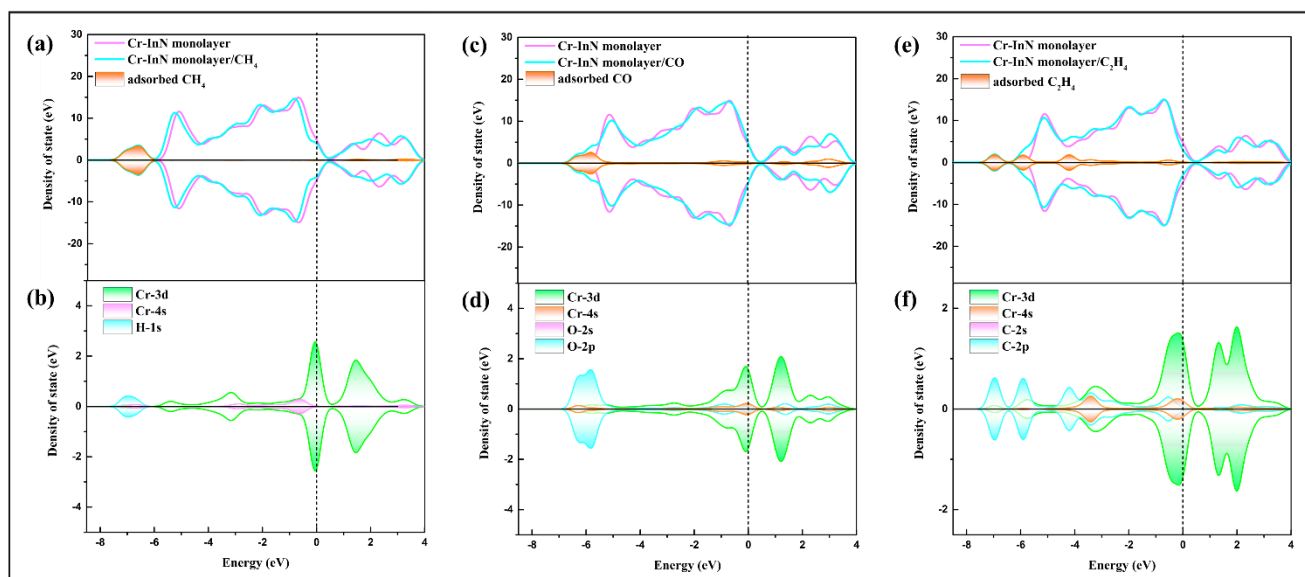

Figure 6. TDOS of (**a**) Cr-InN/CH_4, (**c**) Cr-InN/CO, and (**e**) Cr-InN/C_2H_4; PDOS of (**b**) Cr-InN/CH_4, (**d**) Cr-InN/CO, and (**f**) Cr-InN/C_2H_4 adsorption systems.

First of all, for the CO and C_2H_4 system (identical except for some new states brought about by the introduction of CO and C_2H_4 molecules), the degree of overlap of the TDOS curve before and after adsorption was found to be quite high—the curve near the Fermi level, especially, was almost completely fitted. In PDOS, the O-2p orbital of the CO molecule and the Cr-3d and Cr-4s orbitals of the Cr atom overlapped around -6 eV and between 1 and 4 eV; similarly, there was also overlap between the C-2p orbital of the C_2H_2 molecule and the outer orbital of the Cr atom, manifesting the hybridization phenomenon between the O, C, and Cr atoms. In light of the aforementioned discussion of adsorption energy and electron density, it is believed that CO and C_2H_4 molecules were firmly captured by the Cr–InN monolayer, which was also verified by PDOS analysis. However, the adsorption behaviors of CO and C_2H_4 did not cause drastic changes in the electronic structure near

the Fermi level of the Cr–InN monolayer. That is to say, although the Cr–InN monolayer can adsorb CO and C_2H_4 molecules, it may not produce a remarkable response.

As for the Cr–InN/CH_4 adsorption system, we first paid attention to its PDOS distribution. Similarly to the conclusions obtained from the adsorption energy and charge-transfer analysis, we found that the H-1s atomic orbital in the CH_4 molecule had a slight overlap with the Cr-4s orbital in the range from −8 to −6eV, which again suggests that the CH_4 molecule was present in the Cr–InN monolayer. The chemical bond that was formed was relatively weak. However, the change in TDOS distribution shows that the electronic distribution of the Cr–InN monolayer was remarkably changed by the adsorption of CH_4 molecules. Figure 6a directly shows that the overall state in the adsorption system was low. The energy direction moved, and its energy band seemed to significantly change, that is, the conductivity of Cr–InN may have been reduced due to the adsorption of CH_4.

3.5. Band Structure Analysis

It is widely believed that there is a classic relation between band gap and electrical conductivity [31,32], that is, at a certain temperature, the conductivity is inversely proportional to the band gap. Here, band structure was used to qualitatively analyze the influence of gas adsorption on the band gap of the Cr-doped InN monolayer.

We can further explore the response of the intrinsic Cr–InN monolayer to the adsorption behavior of the three gases through the band structure of the Cr–InN monolayer system shown in Figure 7. Before adsorption, the band gap of the Cr–InN monolayer was 0.683 eV, and after the adsorption of CH_4, CO, and C_2H_4 gas, it dropped to 0.560, 0.598, and 0.615 eV, respectively. This phenomenon is consistent with the conclusion obtained from the analysis of the density of states; the Cr–InN monolayer, that is, the response of the Cr–InN monolayer to CH_4, far exceeded that of the other two gases. Accordingly, a gas sensor based on a Cr–InN monolayer could be developed to achieve the selective detection of CH_4 gas. Additionally, considering the excellent adsorption capacity of the Cr–InN monolayer for CO and C_2H_4 molecules and the harmfulness of CO and C_2H_4, a Cr–InN monolayer could also be developed as an adsorbent for clearing these two gases.
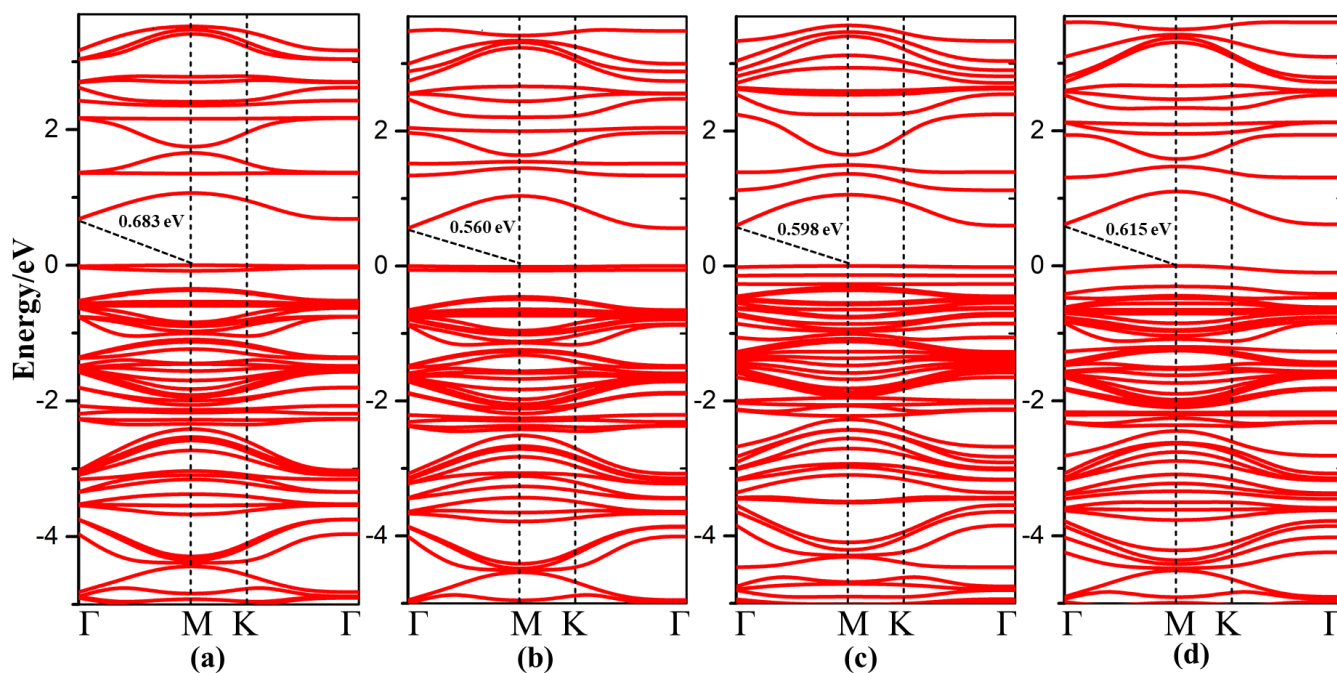

Figure 7. The band structures of the (**a**) Cr-InN monolayer, (**b**) Cr-InN/CH_4, (**c**) Cr-InN/CO, and (**d**) Cr-InN/C_2H_4 adsorption systems at the PBE level in the first Brillouin zone. The first Brillouin zone with high-symmetry k points: Γ (0, 0, 0), M (0.5, 0, 0), and K (0.333, 0.333, 0).

4. Discussion and Conclusions

For this paper, a Cr-doped InN monolayer model was constructed, and based on this model, the adsorption performance of the three characteristic dissolved gases CO, CH_4, and C_2H_4 were calculated. Through the calculation and analysis of adsorption energy, electron density, density of state, and energy band, the following conclusions were obtained:

(1) The Cr–InN monolayer was found to have an excellent adsorption performance to C_2H_4 and CO, while its adsorption effect for CH_4 was found to be relatively ordinary.
(2) Despite the excellent adsorption properties of the Cr–InN monolayer for CO and C_2H_4, the response of the Cr–InN monolayer to these two gases was found to be far from satisfactory. In contrast, the adsorption behavior of CH_4 molecule was found to lead to a more sensitive response.
(3) We advise that the Cr–InN monolayer be exploited as a substrate material of a selective detector for CH_4 and a new type of adsorbing material for treating CO and C_2H_4 gases.

Author Contributions: Conceptualization, G.Q. and J.H.; methodology, W.D.; software, G.Q. and S.W.; data curation, G.Q. and J.H.; writing—original draft preparation, G.Q.; writing—review and editing, G.Q. and Q.Z.; supervision, Q.Z.; project administration, Q.Z. All authors have read and agreed to the published version of the manuscript.

Institutional Review Board Statement: Not applicable.

Informed Consent Statement: Not applicable.

Data Availability Statement: Not applicable.

Conflicts of Interest: We confirm that the authors had no known competing financial interest or personal relationships that could have influenced the work reported in this paper.

References

1. Wani, S.A.; Rana, A.S.; Sohail, S.; Rahman, O.; Parveen, S.; Khan, S.A. Advances in DGA based condition monitoring of transformers: A review. *Renew. Sustain. Energy Rev.* **2021**, *149*, 111347. [CrossRef]
2. Liao, R.J.; Feng, Y.; Yang, L.J. Study on Generation Rate of Characteristic Products of Oil-paper Insulation Aging. *Proc. CSEE* **2008**, *4*, 142–147.
3. Lopes, S.M.D.; Flauzino, R.A.; Altafim, R.A.C. Incipient fault diagnosis in power transformers by data-driven models with over-sampled dataset. *Electr. Power Syst. Res.* **2021**, *201*, 107519. [CrossRef]
4. Jin, L.F.; Chen, W.G.; Tang, S.R. Metal-doped SnO_2 based H_2/C_2H_2 gas sensor array and its detection characteristics. *Chin. J. Sci. Instrum.* **2019**, *40*, 144–152.
5. Tran, D.; Mac, H.; Tong, V.; Tran, H.A.; Nguyen, L.G. A LSTM based framework for handling multiclass imbalance in DGA botnet detection. *Neurocomputing* **2018**, *275*, 2401–2413. [CrossRef]
6. Cui, H.Z.; Yang, L.Q.; Zhu, Y.W.; Li, S.T.; Abu-Siada, A.; Islam, S. A Dissolved Gas Analysis for Power Transformers within Distributed Renewable Generation-Based Systems. *IEEE Trans. Dielectr. Electr. Insul.* **2021**, *28*, 1349–1356. [CrossRef]
7. Zhang, X.X.; Yu, L.; Gui, Y.G.; Hu, W.H. First-principles study of SF_6 decomposed gas adsorbed on au-decorated graphene. *Appl. Surf. Sci.* **2016**, *367*, 259–269. [CrossRef]
8. Diego, C.A.; Nery, V.E.; Daniela, E.O. Fe–doped graphene nanosheet as an adsorption platform of harmful gas molecules (CO, CO_2, SO_2 and H_2S), and the co–adsorption in O_2 environments. *Appl. Surf. Sci.* **2018**, *427*, 227–236.
9. Yao, W.; Zhou, S.; Wang, Z.; Lu, Z.; Hou, C. Antioxidant behaviors of graphene in marine environment: A first–principles simulation. *Appl. Surf. Sci.* **2020**, *499*, 143962. [CrossRef]
10. Zhang, X.X.; Fang, R.X.; Chen, D.C.; Zhang, G.Z. Using Pd-Doped γ-Graphyne to Detect Dissolved Gases in Transformer Oil: A Density Functional Theory Investigation. *Nanomaterials* **2019**, *9*, 1490. [CrossRef]
11. Sun, S.S.; Meng, F.C.; Wang, H.Y.; Wang, H. Novel two-dimensional semiconductor SnP_3: Highest ability, tunable bandgaps and high carrier mobility explored using first-principles calculations. *Mater. Chem.* **2018**, *6*, 11890. [CrossRef]
12. Chen, D.C.; Zhang, X.X.; Xiong, H.; Tang, J.; Xiao, S.; Zhang, D.Z. A First-Principles Study of the SF_6 Decomposed Products Adsorbed Over Defective WS_2 Monolayer as Promising Gas Sensing Device. *IEEE Trans. Device Mater. Reliab.* **2019**, *19*, 473–483. [CrossRef]

13. Liu, Y.P.; Zhou, Q.; Mi, H.W.; Wang, J.X.; Zeng, W. Gas-sensing mechanism of Cr doped SnP$_3$ monolayer to SF$_6$ partial discharge decomposition components. *Appl. Surf. Sci.* **2021**, *546*, 149084. [CrossRef]

14. Rajput, K.; He, J.; Frauenheim, T.; Roy, D.R. Monolayer PC$_3$: A promising material for environmentally toxic nitrogen-containing multi gases. *J. Hazard. Mater.* **2022**, *422*, 12761. [CrossRef]

15. Wang, Y.J.; Zhou, Y.; Wang, Y.H.; Zhang, R.J.; Li, J.; Li, X.; Zang, Z.G. Conductometric room temperature ammonia sensors based on titanium dioxide nanoparticles decorated thin black phosphorus nanosheets. *Sens. Actuators B-Chem.* **2021**, *349*, 130770. [CrossRef]

16. Wang, J.C.; Zhang, X.X.; Liu, L.; Wang, Z.T. Dissolved gas analysis in transformer oil using Ni-Doped GaN monolayer: A DFT study. *Superlattices Microst.* **2021**, *159*, 107055. [CrossRef]

17. Cui, H.; Liu, T.; Zhang, Y.; Liu, Y.X.; Zhou, Z.P. Ru-InN monolayer as a gas scavenger to guard the operation status of SF$_6$ insulation devices: A firstprinciples theory. *IEEE Sens. J.* **2019**, *19*, 5249–5255. [CrossRef]

18. Guo, Y.H.; Zhang, Y.M.; Wu, W.X. Transition metal (Pd, Pt, Ag, Au) decorated InN monolayer and their adsorption properties towards NO$_2$: Density functional theory study. *Appl. Surf. Sci.* **2018**, *455*, 106–144. [CrossRef]

19. Suski, T.; Schulz, T.; Albrecht, M.; Wang, X.Q.; Gorczyca, I.; Skrobas, K.; Svane, A. The discrepancies between theory and experiment in the optical emission of monolayer In (Ga) N quantum wells revisited by transmission electron microscopy. *Appl. Phys. Lett.* **2014**, *104*, 182103. [CrossRef]

20. Zhou, L.; Dimakis, E.; Hathwar, R.; Aoki, T.; Smith, D.J.; Moustakas, T.D.; McCartney, M.R. Measurement and effects of polarization fields on one-monolayer- thick InN/GaN multiple quantum wells. *Phys. Rev. B* **2013**, *88*, 125310. [CrossRef]

21. Sun, X.; Yang, Q.; Meng, R.S.; Tan, C.J.; Liang, Q.H.; Jiang, J.K.; Ye, H.Y.; Chen, X.P. Adsorption of gas molecules on graphene-like InN monolayer: A first-principle study. *Appl. Surf. Sci.* **2017**, *404*, 291–299. [CrossRef]

22. Kohn, W.; Sham, L.J. Self-Consistent Equations Including Exchange and Correlation Effects. *Phys. Rev.* **1965**, *140*, A1133. [CrossRef]

23. Hohenberg, P.; Kohn, W. Inhomogeneous Electron Gas. *Phys. Rev.* **1964**, *136*, B864. [CrossRef]

24. Chen, D.C.; Zhang, X.X.; Tang, J.; Cui, Z.L.; Cui, H. Pristine and Cu decorated hexagonal InN monolayer, a promising candidate to detect and scavenge SF$_6$ decompositions based on first-principle study. *J. Hazard. Mater.* **2019**, *363*, 346–357. [CrossRef] [PubMed]

25. Wang, J.X.; Zhou, Q.; Zeng, W. Competitive adsorption of SF$_6$ decompositions on Ni-doped ZnO (100) surface: Computational and experimental study. *Appl. Surf. Sci.* **2019**, *479*, 185–197. [CrossRef]

26. Gui, Y.G.; Tang, C.; Zhou, Q.; Xu, L.N.; Zhao, Z.Y.; Zhang, X.X. The sensing mechanism of N-doped SWCNTs toward SF$_6$ decomposition products: A first-principle study. *Appl. Surf. Sci.* **2018**, *440*, 846–852. [CrossRef]

27. Wang, J.X.; Zhou, Q.; Xu, L.N.; Gao, X.; Zeng, W. Gas sensing mechanism of transformer oil decomposed gases on Ag-MoS$_2$ monolayer: A DFT study. *Physica E* **2020**, *118*, 113947. [CrossRef]

28. Liu, Y.P.; Zhou, Q.; Hou, W.J.; Li, J.; Zeng, W. Adsorption properties of Cr modified GaN monolayer for H$_2$, CO, C$_2$H$_2$ and C$_2$H$_4$. *Chem. Phys.* **2021**, *550*, 111304. [CrossRef]

29. Liu, Y.P.; Zhou, Q.; Wang, J.X.; Zeng, W. Cr doped MN (M = In, Ga) monolayer: A promising candidate to detect and scavenge SF$_6$ decomposition components. *Sens. Actuators A-Phys.* **2021**, *330*, 112854. [CrossRef]

30. He, X.; Gui, Y.G.; Xie, J.F.; Liu, X.; Wang, Q.; Tang, C. A DFT study of dissolved gas (C$_2$H$_2$, H$_2$, CH$_4$) detection in oil on CuO-modified BNNT. *Appl. Surf. Sci.* **2020**, *500*, 144030. [CrossRef]

31. Du, J.G.; Jiang, G. First-principle study on monolayer and bilayer SnP$_3$ sheets as the potential sensors for NO$_2$, NO, and NH$_3$ detection. *Nanotechnology* **2020**, *31*, 325504. [CrossRef] [PubMed]

32. Cui, H.; Zhang, X.X.; Li, Y.; Chen, D.C.; Zhang, Y. First-principles insight into Ni-doped InN monolayer as a noxious gases scavenger. *Appl. Surf. Sci.* **2019**, *494*, 859–866. [CrossRef]